Characterization of ultra-low permeability tight sandstone reservoir properties and criteria for hydrocarbon accumulation in Chang 6 member, Huaqing area, Ordos basin

Jianbo Liao[1,2]*, Liang Hong[1], Zhiyong Li[1,2], Kaijun Tan[1], Leyi Zhao[3], Jun Yang[3] and Pinghui Yu[1]

[1]Research Institute of Petroleum Exploration and Development Northwest Branch, Lanzhou, China, [2]Key Laboratory of Reservoir Description, CNPC, Lanzhou, China, [3]Exploralion & Development, PetroChina Yunmen Oil field Company, Jiuquan, China

How to accurately predict hydrocarbon enrichment and high-yield areas in ultra-low permeability sandstone reservoirs is a hot spot in petroleum geology. Taking the Chang 6 Member of the Yanchang Formation in the Huaqing Area, Ordos Basin as an example, the quantitative characterization and classification criteria of ultra-low permeability sandstone reservoir properties are systematically studied. The research results show that the seismic reflection characteristics of the Chang 6 Member show multi-stage wedge progradation characteristics, reflecting the sedimentary characteristics of the end of the delta front. The maturity of the minerals in the Chang 6 Member sandstones in the study area is very low, it indicates a low degree of transformation of sediments. Three types of sand bodies, namely sandy debris flow, turbidite, and slump rock sand bodies, were identified in the Chang 6 Member of the Yanchang Formation. The pore types of the Chang 6 Member in the study area include intergranular pores, dissolution pores (feldspar, detrital dissolution pores), and intercrystalline pores. Among them, the intergranular pores and feldspar dissolution pores are the most important storage spaces. The study also found that the test oil production is highly correlated with the cumulative thickness of the massive sandstone segments. Therefore, massive sandstone (sand debris flow) is the main contributor to oil well production, and its distribution directly controls the accumulation of oil reservoirs and the high production of oil wells. In addition, geological parameters affecting reservoir enrichment evaluation were analyzed, which include permeability, oil layer thickness, resistivity, and reservoir penetration rate. Finally, the evaluation criteria for hydrocarbon enrichment in the Chang 6 Member were formulated by the analysis of dominant facies, lithologic assemblages and electrical properties.

1 Introduction

A large amount of tight sandstone oil resources are present in the Yanchang Formation in the Ordos Basin, China. With the deepening of oil and gas exploration and production, relatively high-quality reserves have been utilized to a high degree. Furthermore, the proportion of low-grade hydrocarbon-bearing blocks in untapped geological reserves is increasing. The exploration and development of ultra-low permeability reservoirs with permeability less than 1 millidarcy has become an important part of the rapid growth of reserves and production in the Yanchang Formation (He et al., 2008; Huang et al., 2019; Wang et al., 2022).

The permeability range of ultra-low permeability reservoirs is less than 1.0 mD (Yang et al., 2010; Li et al., 2013; Li, 2022). How to predict high-yield areas in ultra-low permeability sandstone reservoirs has become the focus of attention. In this paper, taking the Chang 6 Member of the Yanchang Formation in the Huaqing Area, Ordos Basin as an example, the quantitative characterization and classification criteria of ultra-low permeability sandstone reservoir properties are systematically studied. This study can provide a reference for formulating reasonable tight sandstone oil reservoir development strategies.

2 Geological background

The Huaqing Oilfield is located in the southwest part of the Ordos Basin (Figure 1). The surface of this area is covered by the Quaternary loess with a thickness of 100–200 m. The surface elevation is 1350–1660 m, and the relative height difference is about 310 m. The proven reserves of the Chang 6 reservoir in the Huaqing Oilfield have reached 500 million tons, with a total resource scale of nearly 1 billion tons. Therefore, the development prospect of its
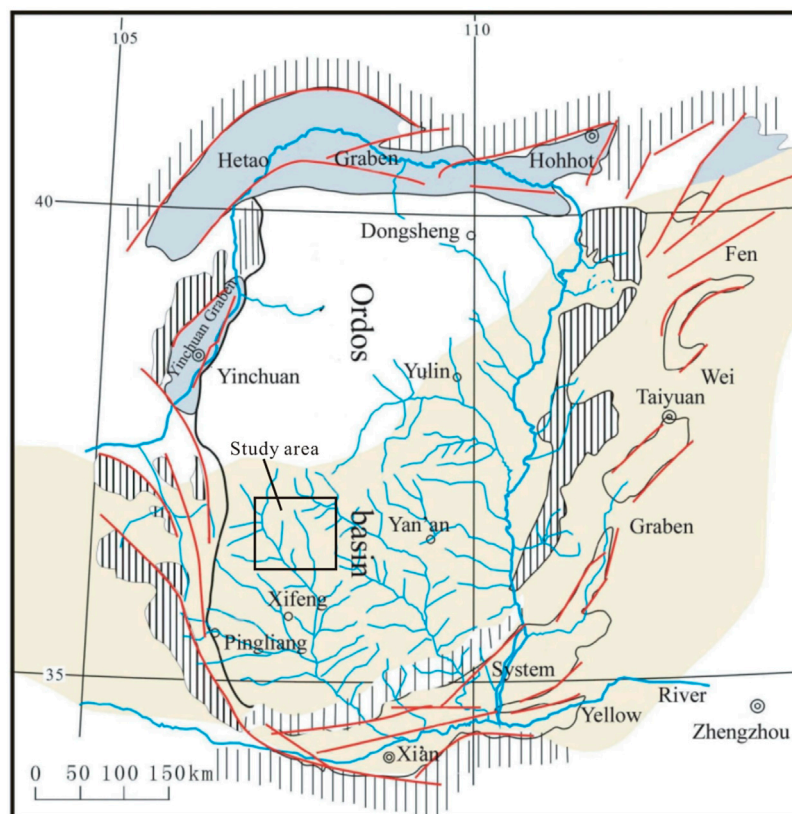

FIGURE 1
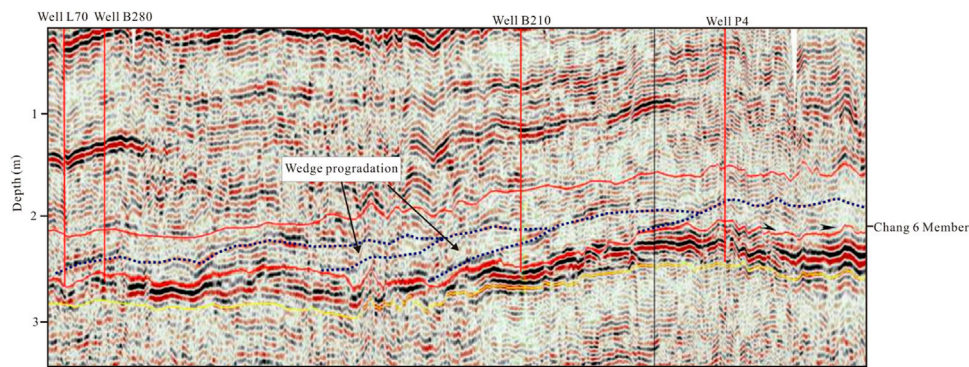Geographical location of the Huaqing area (Liu et al., 2009).

FIGURE 2
A seismic profile passing through Wells L70 and P4 of the study area.

petroleum resources is very broad. There are 121 industrial oil flow wells in the study area, the average oil layer thickness is 10.8 m, the average porosity is 11%, and the average permeability is 0.52 mD. In addition, the average oil test output of a single well is 11.8 t/d, and the daily oil production of the highest producing oil well can reach 119.85 t/d.

3 Databases and methods

Core observation was carried out on 50 drilling cores (about 1100 m in length) in the study area. Physical properties, X-ray diffraction and cast thin sections were tested on the collected samples. The physical property experiments were used to test the porosity and permeability of the samples. The X-diffraction experiments used a Japanese Rigaku DMAX2500X diffractometer. Its 2θ angle measurement range: 10˚ ~ +154˚; scanning step: 0.002˚–90˚ (2θ/θ scanning); 0.001˚–90˚ (2θ scanning); scanning speed: 0.002–100˚/min (2θ/θ scan); 0.001˚–100˚/min (2θ scan). The cast thin section experiments were done with polarized light microscopes, and they were then used to observe the mineral composition, contact relationship, and pore structures within the rock samples. In addition, the petroelectric data and oil testing data of the reservoir were used to analyze the influencing factors of hydrocarbon enrichment.

Based on the comprehensive study of the seismic, geology and well logging, we identified three types of sediment gravity flow and traction bottom flow for the first time in the Chang 6 Member of the Yanchang Formation in Huaqing area, namely, sandy clastic flow, classical turbidite and slump rock sandbodies. Among them, the massive sandy clastic flow is the main oil-bearing reservoir, and the multi-stage vertical superposition constitutes the skeleton sand body of the ultra-low permeability and thick reservoirs.

4 Results

4.1 Sedimentary characteristics of the chang 6 member

It can be seen from the seismic profile that the Yanchang Formation in the study area is relatively flat (Figure 2). For the area near the center of the basin, the Chang 6 Member show multi-stage wedge progradation characteristics, reflecting the sedimentary characteristics of the end of the delta front. The sedimentary slope formed by rapid accumulation provides a prerequisite for the formation of gravity flow slumps.

On the seismic profile, the superposition of the two wedges can be found, which is located at the junction of the end of the delta front and the tail of the gravity flow slump. The event axis reflection in the lower part of the transition zone is clear and continuous. It has a strong lithologic differentiation and can reflect the delta front facies (Liu et al., 2009; Asante-Okyere et al., 2021). However, the reflection of the upper event axis is relatively blurred and internally disordered, showing mixed lithology and strong heterogeneity. It represents the reflection characteristic of the gravitational flow slump facies (Katz et al., 2021; Vafaie et al., 2021; Jiang et al., 2022).

The approximate location of the slope break zone can be determined intuitively by observing the cores of the coring wells on both sides of the slope break. A total of 1100 m of cores were used for core observations. The sedimentary mechanisms of delta front and slump gravity flow are different, which leads to the great differences in the characteristics of their sedimentary structures. The scouring phenomenon of the delta front is obvious, and most of them have the characteristics of tractive flow deposits such as parallel and oblique beddings with coarse lithology (Figure 3). The color of the delta front deposits is mainly light gray or grayish white. However, the slump gravity flow has the characteristics of rapid deposition such as slump
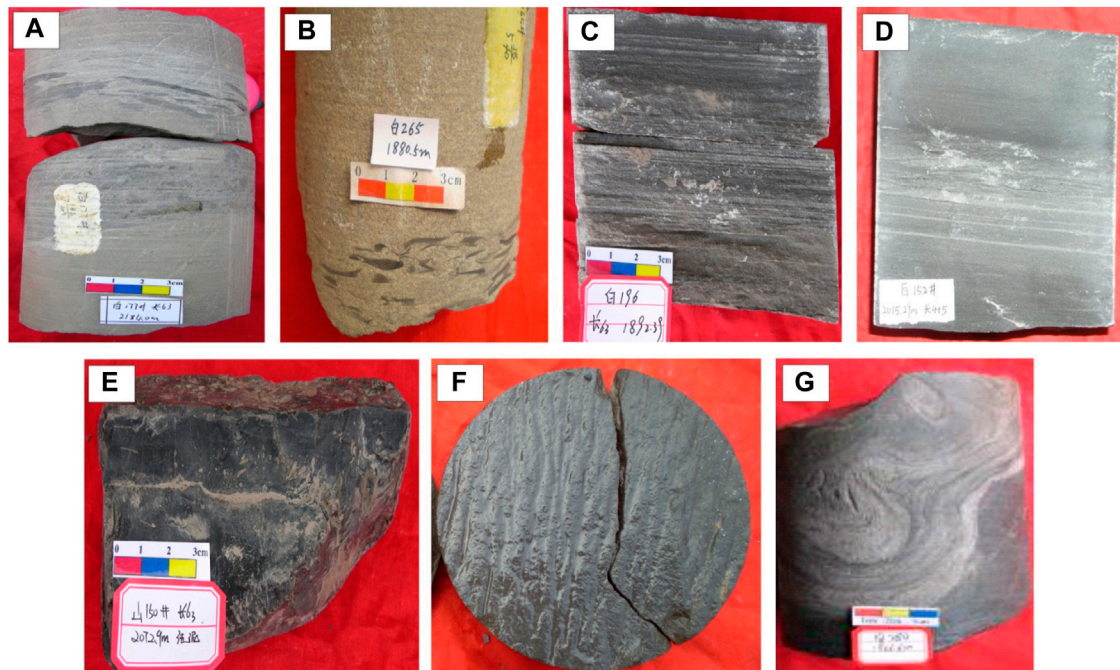
FIGURE 3
Sedimentary-structural characteristics of the Chang 6 Member in the study area. **(A)** Well B177, 2184 m, two-stage channel scour surface; **(B)** Well B265, 1880,5m, scour face contact; **(C)** Well B196, 1892, 39m, parallel bedding; **(D)** Well B152, 2015.29m, oblique bedding; **(E)** Well S150, 2072.9m, deep lake dark mudstone; **(F)** Well H12, 2003m, groove; **(G)** Well H14, 2013m, slump deformation bedding.

deformation, groove mold, slot mold, and heavy-duty mold. Dark mudstone is developed in the slump gravity flows. Meanwhile, the pyrite nodules are common, and it reflects a low-energy and still water depositional environment (Wang, 2005; Zhao et al., 2007; Wu et al., 2008).

Due to the control of paleotopography and sedimentary facies belts, the flow characteristics of the sedimentary medium above and below the slope change significantly. The end of the delta front on the slope belongs to the grain support, and it reflects the transport characteristics of the tractive flow; while the lower slope belongs to the semi-deep lake-deep lake environment, and it has the gravity flow transport characteristics of the matrix support (Figure 3).

4.2 Petrological characteristics of the chang 6 member

The color of rock, especially the primary color of mudstone, can be directly used as an identification marker for judging the climatic conditions, oxidation-reduction conditions of water media and the quality of source rocks during deposition (Tchistiakov, 2000; Zeng et al., 2003; Li et al., 2012). The deep-semi-deep lacustrine facies gray-black to black shales are widely developed in the Chang 6 Member of the study area. It
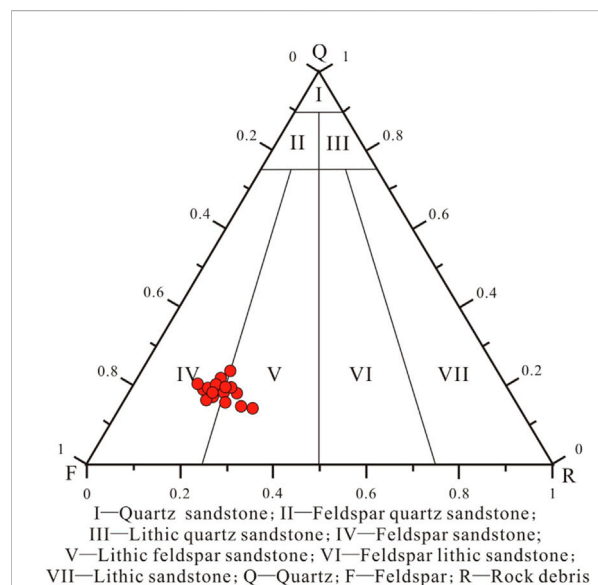

FIGURE 4
Distribution of three-unit components of the Chang 6 sandstone in the study area.

reflects that in the Late Triassic, the study area had perennial water overburden and strong reducing environmental conditions.

The Chang 6 Member of the study area is sandwiched by a large set of dark mudstones. Sandstones and mudstones are interbeded frequently. The clastic composition of sandstone is mainly feldspar and quartz, followed by lithic debris. Its lithology is dominated by powder to fine-grained feldspar sandstone, followed by lithic sandstone, and quartz sandstone is rare to be seen. The three-component distribution of the sandstones is shown in Figure 4. The compositional characteristics of the detrital skeleton components are as follows:

Quartz (Q): It is mainly composed of single crystal quartz, while polycrystalline quartz is occasionally seen, and siliceous debris is not seen. The content of quartz is between 18 and 40%, mainly 25–30%, and the average is 28%.

Feldspar (F): It is dominated by plagioclase, followed by striped feldspar, microplagioclase, and a small amount of albite and orthoclase. According to the identification results of thin sections, the content of feldspar is between 41% and 74%, mainly 50%–60%, and the average is 61.7%. The albite component is slightly dominant.

Rock debris (R): The types of rock debris are relatively complex. It is mainly composed of epimetamorphic rock debris, including phyllite, metasiltstone, mica-quartz schist, and quartz-mica schist; followed by sedimentary rock debris, including micrite limestone, micrite dolomite, calcite debris, dolomite debris, flint debris; and the intermediate-basic magmatic rock debris is occasionally seen. The total content of various types of debris is between 3% and 34%, mainly 6%–16%, and the average is 10.2%.

Therefore, the mineral maturity of the Chang 6 Member sandstone in the study area is very low, indicating that the sedimentary environment has a low degree of transformation of the sediments. It is the product of the rapid promiscuous accumulation of sediments.

4.3 Sand body types in the chang 6 member

Three types of sediment gravity flow and traction bottom flow of sandy clastic flow, classical turbidite and slump rocks were identified in the Chang 6 Member of the Yanchang Formation. Among them, the sandy clastic flow is a kind of sand body genetic type developed in continental petroliferous basins and belongs to laminar flow; while the classical turbidite is formed by turbidite flow and belongs to turbulent flow; and the slump rock is a slump deformation body formed by sliding and slumping in deep water environment (Amaefule et al., 1988; Bennion et al., 2000; Jiang et al., 2006).

The above three lithologies are interdependent in space and transform in time. In terms of oil and gas-bearing properties, the sandy clastic flow is the best, followed by the classical turbidite, and the slump rock has the poorest gas-bearing properties (Liao et al., 2018; Liao et al., 2020). Further research shows that the sandy debris

flow is the main contributor to the production of oil wells in the central areas of the lake basin, and its planar distribution controls the enrichment and high production of oil and gas.

Statistical analysis results of 200 samples from the Chang 6 Member of this area show that, compared with the channel sand bodies of the traction flows in the same period, the gravity flow sand bodies generally have higher content of matrix and poor overall storage performance, and the permeability of most samples is lower than 0.5 mD. On the whole, the physical properties of the sandy clastic flow reservoirs are better than those of turbidite, and the slump rocks have the worst physical properties due to the sand-mud mixture. The study of the microstructures of the sandstone reservoirs show that although massive sandstone (sand clastic flow) has a higher content of matrix (hydromica), its physical properties are generally better than the turbidite and slump rocks. Moreover, the sandy debris flow is dominated by the development of intergranular and dissolution pores.

4.4 Provenance of the chang 6 member

There are two provenance systems in the northeast and southwest of the study area, among them, the northeast one is the main source. The provenance demarcation line represents the connecting areas of the Wells Li 60-Bai 181-Hua 93-Bai 282-Cheng 97-Shan 105. The content of feldspar is higher than that of quartz in the northeast direction of the dividing line, while the content of quartz in the southwest direction is higher than that of feldspar.

Under cathode ray irradiation, there are three types of quartz luminescent colors with standard genetic significance: ① Quartz that emits blue-violet light is formed in plutonic or volcanic rocks, and will be rapidly cooled under high temperature above 573°C. ② Quartz with reddish brown and brown light is formed in regional metamorphic rocks with a temperature of 300–573°C, and its cooling rate is relatively "slow". Affected by pressure dissolution, temperature and pressure in diagenesis, authigenic quartz may also emit light brown light. ③ Non-luminous quartz is authigenic quartz formed during diagenesis, and the formation temperature is generally less than 300°C.

The quartz in the Well Bai 209 in the northern part of the Huaqing area emits blue-violet light (Figure 5A), reflecting the original characteristics of the parent rock of the upper-Mesoproterozoic granite gneiss high-grade metamorphic rock series in the Yinshan area. However, the Well Li37 in the south mainly emits brown-red light (Figure 5B), and it reflects the characteristics of the parent rock of the sedimentary rock in the southwestern Qinqi Fold Belt. From the above analysis, it can be seen that the quartz cathodoluminescence has two different regions, indicating that there are two kinds of parent rock sources in the Huaqing area.

The risk of production and construction in the provenance intersection area is relatively high, and the direction of
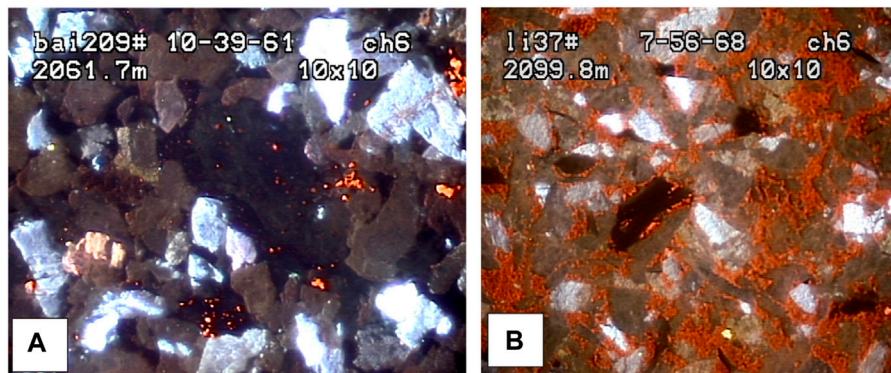
FIGURE 5
Microscope photos of the Chang 6 sandstone in the study area. **(A)** Well Bai 209, quartz has blue-brown-blue luminescence; **(B)** Well Li 37, quartz has brown-red luminescence.
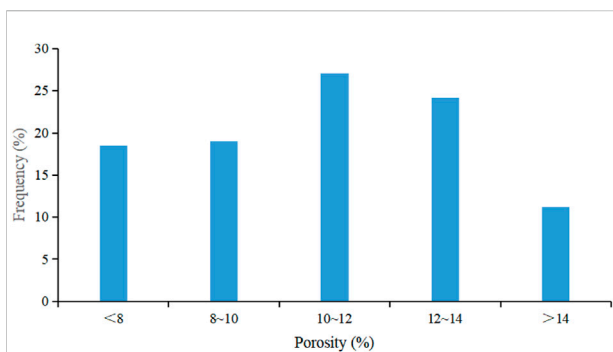

FIGURE 6
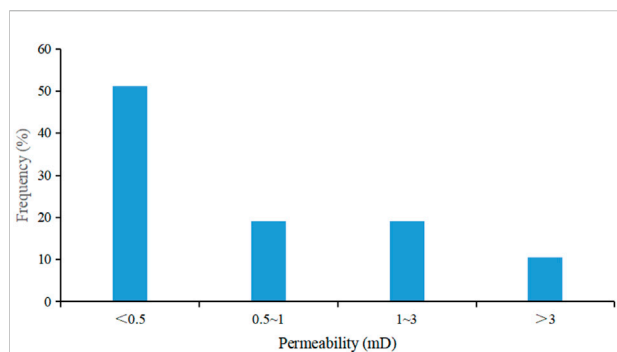Distribution of porosity in the Chang 6 Member of the study area.

FIGURE 7
Distribution of permeability in the Chang 6 Member of the study area.

production and construction should be traced to the massive clastic flow sandstone on the main belt of the gravity flows in the northeast direction. The blocks that have formed commercial production capacity in the Huaqing area are basically in the main belt of gravity flows. Therefore, in the follow-up search for production and construction targets, the main sand belt of gravity flow that spreads from east to west is the main target.

5 Discussion

5.1 Evaluation of thick ultra-low permeability reservoirs

Permeability <1 mD is an ultra-low permeability reservoir. The Yanchang Formation in the Ordos Basin as a whole is a low permeability reservoir. Among them, the porosity of the Chang

6 oil layer group in the study area is generally less than 14%, and such reservoirs account for 88.8% of all samples (Figure 6); the permeability is generally less than 3 mD, and the reservoirs with permeability less than 1 mD account for 70.3% of the total samples (Figure 7).

For different oil layers in the Chang 6 Member, the sand bodies deposited in the late stage (Chang 6_1) have relatively good physical properties. Its average permeability is 1.2 mD. However, the older the horizons, the much pore poor the reservoir physical properties. The permeability of the Chang 6_2 and Chang 6_3 sandstones are 0.91 mD and 0.37 mD, respectively.

The thick sand layers of the Chang 6 Member in the study area are mainly formed by sandy debris flows with liquefied flow properties. The most important feature of the sandy debris flow is its liquefaction origin, and the main sources are the saturated water and fine sediments. After entering the hydrostatic deposition, the sandy debris flow did not carry out secondary

differentiation of sediments in the process of slump along the slope like turbidite, but declined as a whole. In addition, the liquefied property of sandy debris flow is also an important reason for its large single-stage slump thickness (Xu et al., 1999; Peng and Chen, 2013). Generally, the thickness of single-layer sandy debris flow sandstone can reach 10–15 m. In addition, it has the characteristics of multi-stage superposition, so a single well often encounters a sandstone reservoir with a thickness of nearly 40 m.

It is worth noting that the calcareous interlayers are often associated with large sets of thick sandstones in some areas. On the one hand, it is due to the large content of feldspar in the sandstone; on the other hand, it also shows that the later reformation of diagenesis has an important influence on the properties of the reservoir.

The background of near-source rapid deposition results in poor sorting and roundness of ultra-low permeability reservoirs (Bukar et al., 2021). It is mainly supported by matrix, which reflects its weak hydrodynamic environment. It can also be found from the observations under the microscope that a small number of particles have good roundness, while most of the particles have moderate to poor roundness, indicating the effect of secondary transportation. The sandstone is dominated by quartz and feldspar, and the content of feldspar is generally higher than that of quartz, which is very different from most conventional sedimentary reservoirs. On the one hand, it illustrates the alkaline environment of its parent source area; on the other hand, it also reflects the relatively short transport distance of sediment debris from a microscopic perspective (Xu et al., 2013; Zou et al., 2019). Feldspar is much less stable than quartz, and it will cause a lot of losses during long-distance transportation. Under normal circumstances, after entering the lake basin, the content of quartz is greater than that of feldspar, and the phenomenon that feldspar is greater than quartz in the center of the lake basin in Huaqing area is abnormal. From this, it can be judged that the formation of thick ultra-low permeability sandstone in this set of strata is closely related to the nature of its parent source.

A large number of core observations show that the continuous thickness of the sandy debris flows is large and the oil-bearing properties are good. Classical turbidite has a lithologic combination of frequently interbeded of sand and mud. Meanwhile, it has well-developed rhythmic bedding structures, and only some layers have good oil-bearing properties (oil-rich or oil-immersed). However, slump rocks are less oily (oil spots or traces). In order to further determine the oil and gas properties of sand bodies of different genetic types, 82 wells were selected in the Huaqing area, and the correlation between oil production and logging interpretation of the thickness of oil layers and the thickness of massive sandstones (sand clastic flow) was carried out respectively. Statistical results show that the level of oil testing production is highly correlated with the cumulative thickness of the massive sandstones
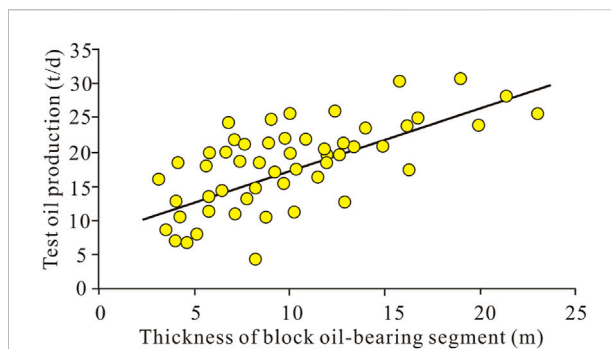

FIGURE 8
Relationship between massive sandstone thickness and oil test production.

(Figure 8). Therefore, the massive sandstone (sand debris flow) is the main contributor to oil well production, and its distribution directly controls the scale of hydrocarbon accumulation.

5.2 Analysis of pore types in ultra-low permeability reservoirs

According to the mercury injection test results of the Chang 6 Member of the Wells Bai 210–27 and Bai 209, the oil layer displacement pressure is 1.27 MPa, the median pressure is 7.52 MPa, the median radius is 0.11 μm, the maximum mercury injection saturation is 84.12%, and the mercury removal efficiency is 27.0%. The sorting of throats is good with the average sorting coefficient of 2.15, and small pores and fine throats are developed in the ultra-low permeability reservois.

The reservoir pore types of the Chang 6 Member in the study area include intergranular pores, dissolution pores (feldspar, detrital dissolution pores) and intercrystalline pores. Among them, intergranular and feldspar dissolution pores are the most important storage spaces in the Chang 6 Member sandstones (Figure 9).

1) Intergranular pores: This type of pores is the most important and common type of pores in the sandstone. The intergranular pores in the Chang 6 reservoir account for about 60% of the total surface porosity.
2) Feldspar dissolution pores: This kind of pores were formed by the dissolution of feldspar grains, and they belong to secondary pore type that developed in delta sedimentary bodies. The feldspar dissolved pores that developed in the Chang 6 reservoir account for 12–18% of the total surface porosity.
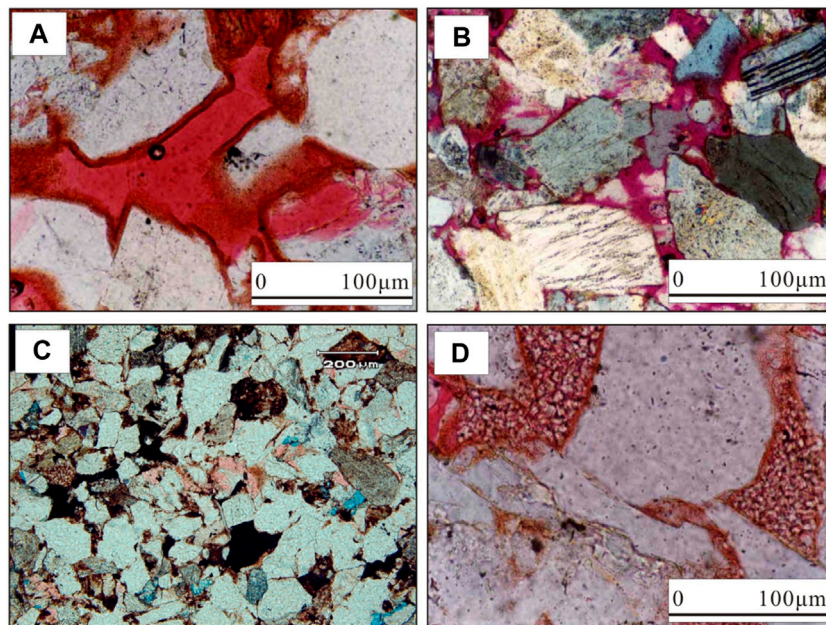3) Laumontite dissolution pores: It is the secondary pores formed by the dissolution of the laumontite dissolution

FIGURE 9
Main pore types that developed in the Chang 6 sandstones in the study area. **(A)** Well A8, 2190.42m, the pore combination of dissolution pores and intergranular pores; **(B)** Well Ping 40−20, 1167.84m, the laumontite was strongly dissolved; **(C)** Well Zhuang 33, 1678.38m, feldspar dissolution pores; **(D)** Well A14, 2133.50m, kaolinite intercrystalline pores.
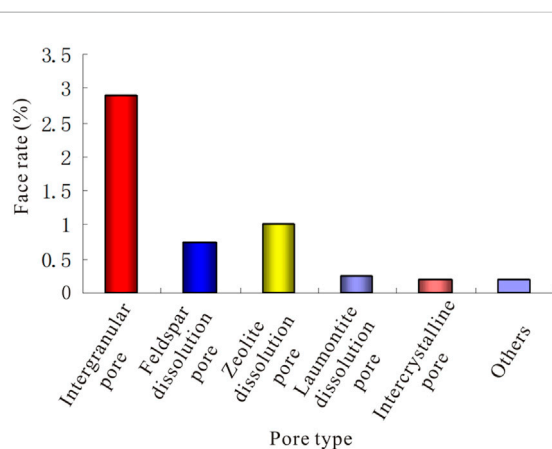

FIGURE 10
Pore types and proportions in the sandstone of the Chang 6 Member in the study area.

pores filled between the detrital particles or of the metasomatic detritus. Laumontite dissolution pores are commonly developed in the Chang 6 reservoirs, generally accounting for 10–20% of the total pore porosity, and their absolute content is 1.0% (Figure 10).

4) Intercrystalline pores and debris dissolution pores: The contribution of these two types of pores to the
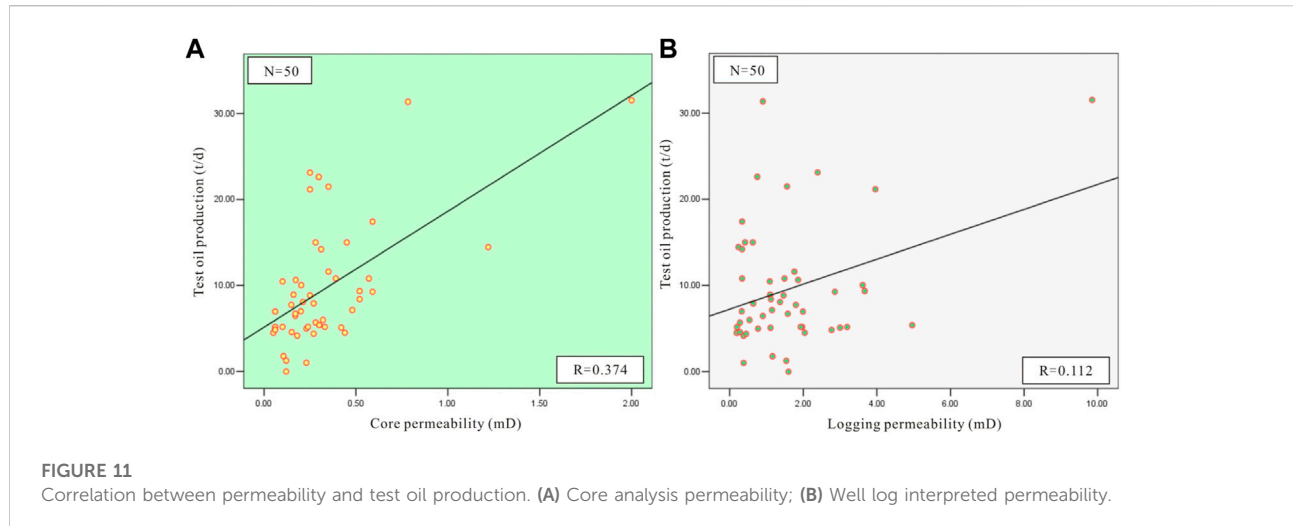
improvement of reservoir physical properties is relatively small, and their contribution to pore spaces generally located in intervals where turbidite is not developed.

5.3 Analysis of geological parameters affecting hydrocarbon enrichment

5.3.1 Permeability

In ultra-low permeability reservoirs, permeability is one of the important parameters that can reflect the essential properties of the reservoir. In the production process, the most easily obtained permeability results are calculated from the logging parameters. However, in practical applications, these results often deviate greatly from the actual situation. Different calculation standards and methods can also lead to different results for the same reservoir or similar results between different reservoirs. Clearly, none of these conditions can correctly reflect the changes of permeability of the reservoir.

The permeability obtained by the core analysis experiments is the actual reflection of the permeability of the core. However, due to the needs of economic benefits and production efficiency, core analysis is only performed on the exploratory wells, evaluation wells and a small number of skeleton wells in actual production. During the production process, the correlation between actual production and the permeability of core analysis is higher than

FIGURE 11
Correlation between permeability and test oil production. **(A)** Core analysis permeability; **(B)** Well log interpreted permeability.

that of logging interpretations (Figure 11). Therefore, how to accurately reflect the real permeability of the reservoir without increasing production input has become an urgent need in the process of the actural geological research.

Spontaneous potential is one of the important logging parameters to measure reservoir permeability. In the early days of resistivity logging, a non-artificial DC potential difference was observed in drilling, and it could be recorded with millivolt precision, which is called spontaneous potential. The measurement of spontaneous potential is very simple, that is, one measuring electrode is placed downhole and the other one is placed on the ground, and a spontaneous potential curve can be measured continuously. If the positive potential of the curve is used as the benchmark, the negative peak of the curve is generally sandstone with permeability. Therefore, the spontaneous potential curve can be used as a basic logging method to divide lithology and judge reservoir properties. But it is affected by mud filtrate, and the potential value between wells cannot be compared.

The obvious anomaly of spontaneous potential is a significant feature of the permeable layers, and the spontaneous potential curve is an effective tool to divide the permeable layers. Generally, the interface of the permeable layers can be determined by the half-amplitude point. In practical work, a permeable layer is often divided by the display of the spontaneous potential and the micro-electrode curve; and the apparent resistivity curve of the micro-electrode and the short electrode is used to determine the interface. It refers to the half-amplitude point of the natural potential.

Therefore, the potential value of the mudstone layer in the middle of the Chang 6 Member, which is stably developed in the whole area, is taken as the baseline. It represents the adsorption capacity to ions of similar mudstones in the whole

area. Assuming that it is a constant value, the potential of the reservoir at the bottom of the Chang 6 Member is calculated by making a difference with it to obtain the potential amplitude. This result reflects the difference in ion adsorption capacity of reservoirs with the same mudstone layer. Furthermore, it objectively reflects the difference in permeability between reservoirs. It was found that the permeability has a high correlation with the potential amplitude (Figure 12). Therefore, the spontaneous potential is an important parameter to measure the permeability of the reservoir.

5.3.2 Thickness of oil layers

Reservoir thickness is an important parameter to measure reservoir scale and its potential. Usually, the thickness of the oil layer is closely related to the crude oil production. In most cases, we use the effective oil layer thickness after logging interpretation as the main standard of oil layer thickness. However, ultra-low permeability reservoirs have the characteristics of low porosity and ultra-low permeability, and their electrical parameters change little. Therefore, the limitation of the span of the parameter range makes it difficult to divide the effective oil layer thickness by conventional logging methods.

To minimize this disadvantage, the reservoirs interpreted by the logs were further sub-categorized. First, a classification template based on oil layers is established, and the Types I and II oil layers are used as the main body of the "main contribution layer" (test oil production >10 t/d). Then, the correlation analysis was carried out on the thicknesses of the main production layers and the oil layers explained by logging and the oil test results (Figure 13). The comparison shows that the correlation between the thickness of the main production layers and the oil test production is much higher than the thickness of the oil
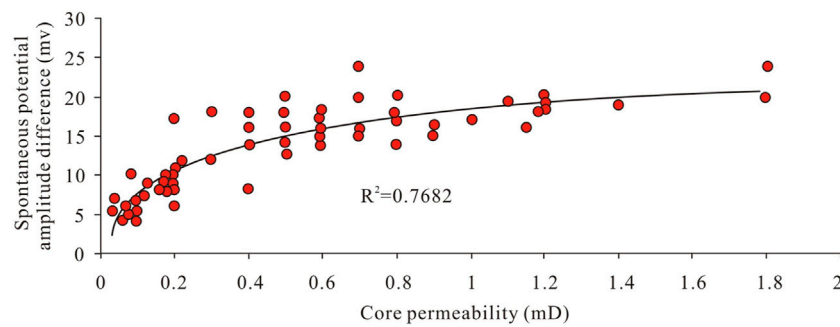
FIGURE 12
Correlation between spontaneous potential amplitude and measured core permeability of the Chang 6 Member in the study area.
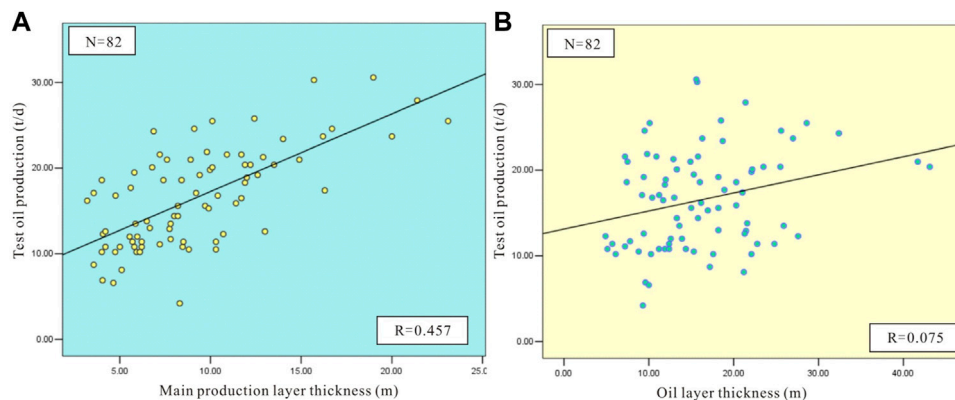

FIGURE 13
Correlation between the thickness of the main producing layers, oil layers and the test oil production in the Chang 6 Member. **(A)** Main producing layer thickness; **(B)** Oil layer thickness.

layers interpreted by logging. Therefore, the thickness of the main production layers is also an important factor affecting the oil content or productivity.

5.3.3 Resistivity

The resistivity of rock is closely related to lithology, reservoir physical properties and oil content. The resistivity of the oil layers in the ultra-low permeability reservoirs in the study area is basically between 18–70 $\Omega \cdot m$, except for the low-resistivity oil reservoirs (<25 $\Omega \cdot m$) in some areas of Bai 465 development zone, while the average value of resistivity in the rest of the areas is more than 30 $\Omega \cdot m$. The oil layer below 30 $\Omega \cdot m$ tends to have relatively poor oil recovery effect. Generally, oil layers with resistances of 40–50 $\Omega \cdot m$ have higher oil production. However, due to the high shale content and the influence of the surrounding rocks of the upper and lower calcareous sandstones, most of the reservoirs exceeding 70 $\Omega \cdot m$ have poor oil content. Therefore, it is not
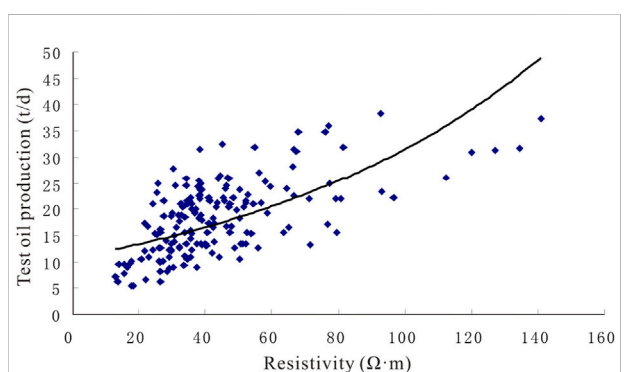

FIGURE 14
Correlation between resistivity and test oil production.

simply considered that the higher the resistivity, the better the oil content, and the resistivity should be within a reasonable range.

TABLE 1 Classification and evaluation criteria of the Chang 6 Member reservoirs in the study area.

Standard\Category	Type I	Type II	Type III
Dominant facies	Turbidite channel facies dominated by a large set of "box-shaped" SP and RT curves	Channel flanks dominated by "bell-shaped or funnel-shaped" SP and RT curves	Sheet sand facies at the outer edge of the channel that dominated by "low-amplitude hill type" SP and RT curves
Lithologic assemblage	Oil-bearing fine sandstone with small trough-like cross-bedding or massive bedding	Massive oil-bearing fine sandstone siltstone and a small amount of thin argillaceous and calcareous interlayers	Cross-bedded fine sandstone
Electrical characteristics	$RT > 40$ Ωm, SPAmplitude < -28 mv, $H > 10$ m	28 Ωm $< RT < 40$ Ωm, $-28 < SP$Amplitude < -12 mv, $5 < H < 10$ m	$RT < 28$ Ωm, SPAmplitude < -12 mv, $H < 5$ m

RT-resistivity; $SP_{Amplitude}$-spontaneous potential amplitude difference; H oil layer thickness.

In this study, the resistivity values of nearly 200 oil-producing wells in the Bai 153 development area were used to analyze the correlation between the resistivity value and the test oil production, and the correlation degree was close to 60% (Figure 14). The conclusion is consistent with the actual logging interpretations in the development process. Therefore, resistivity is an important parameter affecting oil-bearing properties of ultra-low permeability reservoirs (Figure 14). For tight sandstones, high resistivity represents low water saturation and good hydrocarbon-bearing properties.

5.3 4 Drilling encounter rates of oil layers

Drilling encounter rates refer to the probabilities of encountering oil formations during drilling. A formation with a low oil layer drilling encounter rate cannot be called a main productive oil layer in terms of its scale and integrity, and even if its reservoir physical properties are good. According to the research, it has no obvious correlation with production. However, the drill encounter rate can reflect the thickness and connectivity of the sand bodies, so it is also an important indicator of the quality of the oil layers.

5.4 Evaluation criteria for hydrocarbon enrichment

On the basis of the above research, combined with the dominant facies, lithologic combinations and electrical properties, the evaluation criteria for hydrocarbon enrichment in the Chang 6 Member were formulated (Table 1). Using this standard, high-precision prediction of the sweet spot areas of the reservoirs can be achieved. This study can provide scientific guidance for the efficient development of continental ultra-low permeability tight sandstone oil reservoirs.

6 Conclusion

1) Three types of sand bodies, namely sandy debris flow, turbidite and slump rock, were identified in the Chang 6 Member of the Yanchang Formation in the study area. The pore types of the Chang 6 Member in the study area include intergranular pores, dissolution pores (feldspar, detrital dissolution pores), and intercrystalline pores. Among them, intergranular pores and feldspar dissolution pores are the most important storage spaces in the target layer.

2) The study found that the test oil production is highly correlated with the cumulative thickness of the massive sandstone segments. Therefore, massive sandstone (sand debris flow) is the main contributor to oil well production, and its distribution directly controls the accumulation of hydrocarbons and the high production of oil wells.

3) Geological parameters affecting reservoir enrichment include the permeability, oil layer thickness, resistivity, and reservoir penetration rate. The evaluation criteria for hydrocarbon enrichment in the Chang 6 Member were formulated combining the analysis of dominant facies, lithologic assemblages and electrical properties.

Data availability statement

The original contributions presented in the study are included in the article/supplementary material, further inquiries can be directed to the corresponding author.

Author contributions

JL is responsible for the idea and writing of this paper and LH, ZL, KT, LZ, JY and PY are responsible for the experiments and analysis.

Funding

Conflict of interest

Authors JL, LH, ZL, KT and PY were employed by the Research Institute of Petroleum Exploration and Development Northwest Branch, and authors LZ and JY were employed by the PetroChina Yunmen Oil field Company.

Publisher's note

All claims expressed in this article are solely those of the authors and do not necessarily represent those of their affiliated organizations, or those of the publisher, the editors and the reviewers. Any product that may be evaluated in this article, or claim that may be made by its manufacturer, is not guaranteed or endorsed by the publisher.

References

Amaefule, J. O., Kersey, D. G., Norman, D. L., and Shannon, P. M. (1988). "Advances in formation damage assessment and control strategies," in Proceedings of the 39th Annual Technical Meeting of Petroleum Society of CIM and Canadian Gas Processors Association, Calgary, Alberta, June 11-15, 1988, 12–16. CIM Paper No. 88-39-65. doi:10.2118/88-39-65

Asante-Okyere, S., Ziggah, Y. Y., and Marfo, S. A. (2021). Improved total organic carbon convolutional neural network model based on mineralogy and geophysical well log data. Unconv. Resour. 1, 1–8. doi:10.1016/j.uncres.2021.04.001

Bennion, D. B., Thomas, F. B., and Ma, T. (2000). Formation damage processes reducing productivity of low permeability gas reservoirs. SPE 60325, 1–7. doi:10.2523/60325-MS

Bukar, M., Worden, R., Bukar, S., and Shell, P. (2021). Diagenesis and its controls on reservoir quality of the Tambar oil field, Norwegian North Sea. Energy Geosci. 2 (1), 10–31. doi:10.1016/j.engeos.2020.07.002

He, J., Feng, S. B., Huang, J., Yuan, X. Q., Han, P., and Li, T. Y. (2008). Effects of provenance on porosity development of Chang 6 sandstone of the Yanchang Formation in the center of Ordos Basin. Acta Sedimentol. Sin. 29 (1), 80–87. doi:10.1631/jzus.A1000105

Huang, Y. G., Chen, Z. Q., Wignall, P. B., Grasby, S. E., Zhao, L. S., Wang, X. D., et al. (2019). Biotic responses to volatile volcanism and environmental stresses over the Guadalupian-Lopingian (Permian) transition. Geology 47, 175–178. doi:10.1130/G45283.1

Jiang, H. Q., Yao, J., and Jiang, R. Z. (2006). Reservoir engineering principles and methods. The second edition. Dongying: China University of Petroleum Press, 101–108.

Jiang, W., Zhang, P., Li, D., Li, Z., Wang, J., Duan, Y., et al. (2022). Reservoir characteristics and gas production potential of deep coalbed methane: Insights from the no. 15 coal seam in shouyang block, Qinshui Basin, China. Unconv. Resour. 2, 12–20. doi:10.1016/j.uncres.2022.06.001

Katz, B., Gao, L., Little, J., and Zhao, Y. R. (2021). Geology still matters – unconventional petroleum system disappointments and failures. Unconv. Resour. 1, 18–38. doi:10.1016/j.uncres.2021.12.001

Li, A. R., Wang, W. X., Wu, F. L., Zhao, J. Z., and Zhang, H. (2013). Oil accumulation patterns of Chang 4+5 and Chang 6 in yan'an delta, Ordos Basin. Oil Gas Geol. 34 (5), 667–671. doi:10.11743/ogg20130513

Li, H. (2022). Research progress on evaluation methods and factors influencing shale brittleness: A review. Energy Rep. 8, 4344–4358. doi:10.1016/j.egyr.2022.03.120

Li, S. H., Fang, G. Q., Yang, J. L., Liao, J. B., and Fan, J. M. (2012). Origin of ultra-low permeability reservoirs in Ordos Basin and its significance. Lithol. Reserv. 24 (6), 32–37. doi:10.3969/j.issn.1673-8926.2012.06.008

Liao, J. B., Xi, A. H., Li, Z. Y., Liu, H. Q., Li, X. B., and Wan yan, R. (2018). Microscopic characterization and formation mechanisms of deep-water sandy-debris-flow and turbidity-current sandstones in a lacustrine basin: A case study in the Yanchang Formation of the Ordos Basin, China. Pet. Sci. 15, 28–40. doi:10.1007/s12182-017-0207-9

Liao, J. B., Xi, A. H., Liang, S. J., Zhou, X. P., Li, Z. Y., Di, J., et al. (2020). Genetic mechanisms of deep-water massive sandstones in continental lake basins and their significance in micro–nano reservoir storage systems: A case study of the Yanchang Formation in the Ordos Basin. Nanotechnol. Rev. 9, 489–503. doi:10.1515/ntrev-2020-0040

Liu, C., Zhao, H., and Sun, Y. (2009). Tectonic background of Ordos Basin and its controlling role for basin evolution and energy mineral deposits. Energy Explor. Exploitation 27 (1), 15–27. doi:10.1260/014459809788708219

Peng, S. M., and Chen, Y. Q. (2013). Practical petroleum development geology and reservoir engineering method. Beijing: Petroleum Industry Press, 1–494.

Tchistiakov, A. (2000). Colloid chemistry of in-situ clay-induced formation damage. SPE 58747, 1–5. doi:10.2118/58747-MS

Vafaie, A., Kivi, I. R., Moallemi, S. A., and Habibnia, B. (2021). Permeability prediction in tight gas reservoirs based on pore structure characteristics: A case study from south western Iran. Unconv. Resour. 1, 9–17. doi:10.1016/j.uncres.2021.08.001

Wang, H., Zhou, S., Li, S., Zhao, M., and Zhu, T. (2022). Comprehensive characterization and evaluation of deep shales from Wufeng-Longmaxi Formation by LF-NMR technology. Unconv. Resour. 2, 1–11. doi:10.1016/j.uncres.2022.05.001

Wang, Q. Z. (2005). Research on depositional systems and pool-forming assemblages of Chang 1 and Chang 2 members of the Yanchang Formation from ansai-zichang area in the Ordos Basin. Xi'an: Northwest University, 1–5. doi:10.1016/S1872-5791(08)60056-1

Wu, F. L., Wang, B. Y., Zhao, J. Z., Liu, H. B., Li, G. T., and Chen, M. Q. (2008). Origin and characteristics of oil pool sequence in Ordos Basin. Acta Pet. Sin. 29 (5), 639–643. doi:10.7623/syxb200805002

Xu, G. M., Xu, H. D., and Kong, X. Y. (1999). AppliIcation of high-resolution sequence stratigraphy in reservoir numerical simulation. Oil Gas Geol. 20 (2), 115–119. doi:10.11743/ogg19990204

Xu, L., Shi, Y. M., Xu, C. S., Yang, Y., Li, H., and Chai, Z. (2013). Influences of feldspars on the storage and permeability conditions in tight oil reservoirs: A case study of chang-6 group, Ordos Basin. Petroleum Explor. Dev. 40 (4), 481–487. doi:10.1016/S1876-3804(13)60061-0

Yang, H., Li, S. X., and Liu, X. Y. (2010). Characteristics and resource prospects of tight oil and shale oil in Ordos Basin. Acta Pet. Sin. 34 (1), 1–11. doi:10.7623/syxb201301001

Zeng, D. Q., Zhang, S. M., and Lu, L. Z. (2003). Types and characteristics of fractures in tight sandstone gas reservoirs with low permeability. Acta Pet. Sin. 24 (4), 36–39. doi:10.1007/BF02974893

Zhao, J. Y., Luo, J. L., Lei, X. L., Guo, D. Y., Wang, Y. D., Fan, W. H., et al. (2007). Provenance analysis of the sixth member of the Yanchang Formation in the yangjiayuanze oil prospect area, zichang oilfield, Ordos Basin. Geol. China 34 (3), 422–429. doi:10.1002/pon.1349

Zou, C. N., Zhu, R. K., Chen, Z. Q., Ogg, J. G., Wu, S. T., Dong, D. Z., et al. (2019). Organic-matter-rich shales of China. Earth-Science Rev. 189, 51–78. doi:10.1016/j.earscirev.2018.12.002